Geophysical Research Letters

RESEARCH LETTER
10.1029/2018GL079622

First Evidence of Anoxia and Nitrogen Loss in the Southern Canary Upwelling System

E. Machu[1,2], X. Capet[3,2], P. A. Estrade[2], S. Ndoye[2], J. Brajard[3], F. Baurand[4], P.-A. Auger[1,5], A. Lazar[3,2], and P. Brehmer[6]

[1]Laboratoire d'Océanographie Physique et Spatiale (LOPS), IUEM, Univ. Brest, CNRS, IRD, Ifremer, Brest, France, [2]Laboratoire de Physique de l'Atmosphère et de l'Océan Siméon Fongang (LPAOSF), Ecole Supérieure Polytechnique, Université Cheikh Anta DIOP, Dakar, Sénégal, [3]Laboratoire d'Océanographie et du Climat: Expérimentations et Approches Numériques (LOCEAN), UMR7159-CNRS/IRD/UPMC, Paris, France, [4]Instrumentation, Moyens Analytiques, Observatoires en Géophysique et Océanographie, US191-IRD, Technopole Brest Iroise, Plouzané, France, [5]Instituto Milenio de Oceanografía (IMO) and Escuela de Ciencias del Mar, Pontificia Universidad Católica de Valparaíso, Valparaíso, Chile, [6]Institut de Recherche pour le Développement (IRD), UMR LEMAR (UBO, CNRS, IRD, Ifremer), Délégation Régional IRD France-Ouest, Campus Ifremer, Plouzané, France

Key Points:
- Nearshore anoxia was detected in the West African shelf despite subsurface waters being more oxygenated than in other eastern boundary systems
- Production of nearshore anoxia events in Senegalese waters involves 3-D dynamics and is plausibly favored during upwelling relaxations
- Nearshore anoxia has potential implications on the nitrogen cycle through fixed nitrogen loss as observations confirm in Senegalese waters

Supporting Information:
- Supporting Information S1

Correspondence to:
E. Machu,
eric.machu@ird.fr

Citation:
Machu, E., Capet, X., Estrade, P. A., Ndoye, S., Brajard, J., Baurand, F., et al. (2019). First evidence of anoxia and nitrogen loss in the southern Canary upwelling system. *Geophysical Research Letters*, *46*, 2619–2627. https://doi.org/10.1029/2018GL079622

Received 3 AUG 2018
Accepted 23 JAN 2019
Accepted article online 28 JAN 2019
Published online 1 MAR 2019

Abstract The northeastern Atlantic hosts the most ventilated subsurface waters of any eastern boundary upwelling system, while coastal upwelling source waters are slightly above hypoxic levels. Anoxic conditions have previously been found offshore inside mesoscale eddies whose core waters undergo oxygen consumption for many months. Based on circumstantial in situ observations, this study demonstrates that the Senegalese coastal ocean is subjected to episodic occurrence of zero dissolved oxygen concentration at depth along with elevated nitrite concentration (11 mmol/m^3) and nitrate/nitrite deficit to phosphate, thereby indicating severe anoxia and intense nitrogen loss. The anoxic event was associated with a prolonged upwelling relaxation episode in March 2012 and a nearshore diatom bloom that underwent degradation while being advected offshore in stratified waters. This is consistent with scenarios observed in other upwelling systems (Benguela and California), and such conditions are presumably frequent in the southern part of the Canary system.

Plain language summary Oxygen is a key requirement for respiration by marine living organisms. Warming of the atmosphere and the ocean surface reduces the oxygenation of offshore waters. Similarly, the extra load of nutrients from agriculture or waste waters modifies algal production, particularly in coastal regions, often resulting in oxygen-depleted waters. Specific reactions affecting the ionic forms of nitrogen also occur within oxygen-depleted waters, which also impact the nitrogen cycle by generating nitrite, which is poisonous for marine organisms, and nitrous oxide, a powerful greenhouse gas. We took measurements at sea to show that a poorly studied coastal sector of the North Atlantic Ocean, the Senegalese continental shelf, can be episodically subjected to complete depletion of subsurface oxygen (anoxia) as well as high nitrite concentrations, constituting the first report of anoxia for this oceanic region. We also show that this anoxia is likely the consequence of the decay of a bloom of diatoms, a group of microalgae common in this type of ecosystem that initially developed in shallow waters and transported offshore by anomalous currents associated with low-wind conditions.

1. Introduction

The dissolved oxygen (O2) concentration in oceanic waters results from physico-chemical and biogeochemical processes. Surface waters are often oversaturated in O2 due to photosynthetic activity while subsurface waters are undersaturated as a result of respiration and degradation of organic matter produced in the surface layer. Large areas of the eastern boundary upwelling systems host subsurface oxygen minimum zones (OMZs), but the level of O2 is variable (Sarmiento & Gruber, 2006). The OMZ of the eastern tropical North Atlantic, located between the well-ventilated subtropical gyre and the equatorial oxygen maximum, is composed of a deep OMZ and a shallow OMZ at about 100 m (60–70 μmol/kg). Advection by zonal jets dominates the oxygen supply to the deep OMZ and may be responsible for the intermediate O2 maximum around 200-m depth, between deep and shallow OMZ (Brandt et al., 2015).

Glessmer et al. (2009) showed that the connection of the Mauritanian-Senegalese upwelling region with the deep OMZ is very weak (only ~1% of the upwelling waters originate in the region in their numerical

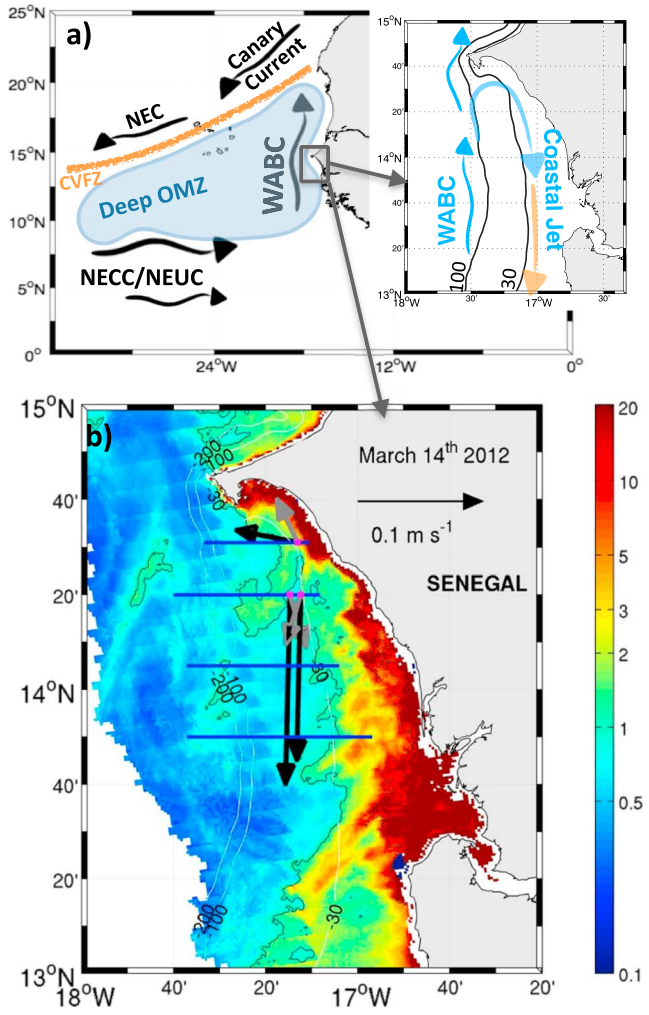

Figure 1. (a) Thermohaline and flow features of the Northeast tropical Atlantic (Arístegui et al., 2009; Kounta et al., 2018) including the Cape Verde frontal zone (CVFZ), North Equatorial Current (NEC), North Equatorial Counter Current (NECC), North Equatorial Undercurrent (NEUC), and West African poleward Boundary Current (WABC). The typical upwelling circulation off southern Senegal is represented in the upper-right panel: The WABC flows northward and feeds the coastal upwelling with nearly hypoxic subsurface waters. The preferential upwelling pathway is situated just south of Dakar. Upwelled water is subsequently advected southward. (b) Surface Chl-a concentrations (mgChl-a/m^3) from Modis Aqua on 14 March 2012. Zonal transects sampled during UPSEN are represented with blue segments. ADCP velocities over the bottom 15 m (resp. near-surface depth range 10 to 5 m) are indicated as black (resp. gray) vectors. The M2 tidal constituent is by far the dominant one. Velocities are time averaged over 4, 1, and 2 M2 periods with final averaging dates and mooring sites (pink square at arrow tails) being, respectively, 5:30 a.m. on 14 March (14.33°N to 17.25°W), 9:00 a.m. on 15 March (14.33°N to 17.21°W), and finally 10:00 p.m. on 16 March (14.52°N to 17.22°W where anoxic Sta-144—pink/blue diamond—was carried out).

experiment). Hence, the deep Atlantic OMZ contributes marginally to low-oxygen events that can occur over the shelf along Senegal and Mauritania. On the other hand, the shallow part of the OMZ is in close proximity to the coastal upwelling region off Mauritania (Brandt et al., 2015; Klenz et al., 2018) and Senegal (Capet et al., 2017). For the latter region, modeling experiments have recently corroborated the existence of mean upwelling pathways conveying offshore waters in the depth/density range of the shallow OMZ from the latitudes of the North Equatorial Countercurrent/Undercurrent to the southern Senegalese shore (Ndoye, 2016; Ndoye et al., 2017; see Figure 1a for the physical regional context).

O2-depleted waters have biological impacts on most marine living organisms. Thresholds of deleterious O2 concentrations vary among classes and species but also depend on the exposure times and frequencies (e.g., Monteiro & van der Plas, 2006; Vaquer-Sunyer & Duarte, 2008). On average, crustaceans are more sensitive than fish, while fish are more sensitive to low O2 levels than bivalves and gastropods. Below 22 μmol/kg extreme stress and mortality of organisms is expected. For example, low-oxygen events have provoked rock lobsters walkout in the southern Benguela (Cockcroft, 2001), the mortality of crabs off Oregon-California (Grantham et al., 2004), and massive fish beaching and mortality off Chile (Hernández-Miranda et al., 2010). While O2 values in the shallow OMZ of the eastern North Atlantic are well above lethal values, hypoxic conditions have been proposed to explain the occasional anomalous mortality of demersal fish (Serranidae) since the late 80s (Caverivière & Touré, 1990; personal communication from investigators of Centre de Recherche Océanographique de Dakar Thiaroye). Nevertheless, no coastal anoxic event has, to our knowledge, been reported in the southern Canary Current System (CCS).

Extreme O2 depletion can also have additional consequences through denitrification and annamox processes by inducing nitrogen loss and/or nitrous oxide (N_2O) outgassing. Such conditions have been identified in different eastern boundary upwelling systems (e.g., Codispoti & Christensen, 1985) including the Benguela (e.g., Kuypers et al., 2005) but has never been reported to occur in the CCS where N_2O is believed to be produced mainly through nitrification pathway (Kock et al., 2012).

A number of studies conducted during the last 15 years show a global deoxygenation trend in both offshore and coastal waters (e.g., Breitburg et al., 2018; Chan et al., 2008). Although the causes of these hypoxia events vary, changes in source waters, wind forcing, and nutrient loading increase are frequently implicated (e.g., Breitburg et al., 2018; Chan et al., 2008; Checkley & Barth, 2009; Diaz & Rosenberg, 2008; Rabalais et al., 2010; Zhang et al., 2010).

This study is, to our knowledge, the first report of extreme deoxygenation and fixed nitrogen loss along the shores of West Africa that are part of the CCS. The field experiment and the data collection and analysis are presented in section 2. Section 3 presents the wind, O2, and chlorophyll-a (hereafter Chl-a) observations available to describe and contextualize the deoxygenation/nitrogen loss episode. A discussion is offered in section 4 on the conditions and processes having led to anoxia and on the broader local to regional implications.

2. Materials and Methods

The UPSEN field experiment took place from 7 to 17 March 2012 on board the FRV Suroît. Observations included 154 CTD stations. Data were acquired using a SBE911+ that measures pressure, temperature, conductivity, fluorescence, and O2 levels. Data postprocessing was performed using the seabird SBE processing software and followed standard practices (see Morison et al., 1994). Ninety-eight samples were analyzed by Winkler method using a iodometric titration with an amperometric endpoint to validate electrochemical O2 concentrations for which the accuracy is ~1.5 μmol/kg (e.g., Aminot & Kérouel, 2004) and the detection limit is 4 μmol/kg (A.Paulmier, pers. com.). Nitrate, nitrite, phosphate, and silicate concentrations were determined with a METROHM Titrino 848 analyzer. Pigment concentrations were measured by high-performance liquid chromatography (Ras et al., 2008, adapted from Van Heukelem & Thomas, 2001; see supporting information S1 caption). The relative percentage of the main phytoplankton taxonomic groups was determined using the diagnostic pigment analysis of Aiken et al. (2009). Multiple short-term deployments of an array of upward looking Acoustic Doppler Current Profilers (ADCP) were made in 30- to 40-m water depths. The array consisted of two RDI (300 kHz) and two AQUADOPP (400 and 600 kHz), each recording currents every 2 min with 1-m bin size. ADCPs were deployed at the northern, southern, western, and eastern ends of a cross, with approximately 1.8-km distance between the extremities. Velocity measurements at the four locations are simply averaged and low-passed filtered (time averaging over one to three M2 tidal periods) to provide estimates of the near-surface and near-bottom subinertial currents at midshelf. The mooring deployments made between 11 and 16 March (respectively, on 16 March) were within 20 km (respectively, 1 km) from where the anoxic observation was made. Wind variability was characterized using data from the Yoff weather station at Dakar Airport (DWS), National Climatic Data Center blended sea winds (Zhang et al., 2006), and wind recorded on board the vessel.

Synoptic sea surface Chl-a concentrations encountered 14 March were provided by Modis Aqua. Data processing involved a specific deconvolution (Diouf et al., 2013) to reduce the contamination due to large amounts of mineral dust in the atmosphere.

3. Results

During UPSEN observation stations were mainly organized along four zonal/across-shore sections situated on the shelf south of Dakar (Figure 1). UPSEN occupied the southernmost section at 13°50′N and 14°06′N, followed by a section at 14°20′N before ending by a section at 14°31′N. Observations described herein focus on the final northern section where hypoxic conditions were encountered over the midshelf and one station (Station 144, hereafter Sta-144) exhibited near-bottom anoxia. Prior to this survey, usual upwelling (northerly) winds of 10–15 knots were blowing over the area (Ndoye et al., 2014). Winds weakened just before the survey started (Figure 2) and blew gently from 7 to 10 March alternating from weak northeasterlies (NE) in the morning to northwesterlies (NW) in the evening (not shown), a usual pattern for this region strongly affected by thermal winds (see Figure 2e in Capet et al., 2017, for the similar diurnal cycle observed in 2013). The relaxation became more pronounced between 10 and 13 March with very weak NW winds punctuated by short periods of weak southerlies. The night and morning of 16 March were marked by alternating NE-NW winds and a southeasterly wind blew over Dakar for an hour at midday. The typical circulation characterized by an equatorward surface-intensified upwelling jet over the midshelf (Figure 1a) reversed to poleward shortly before (Figure 2c). It is during this part of sequence that the observed anoxia developed.

Six stations at depth between 31 and 32 m (127, 130, 134, 144, 148, and 152) were made between 16 March 2:42 a.m. and 17 March 10:10 a.m. within 1 km from 14°31.06′N to 17°13.05′W (hereafter Sta-144). Near-bottom O2 concentrations below ~20 μmol/kg were measured after the 16 at 9:15 a.m. (Sta-130). Among them, Sta-144 exhibited pronounced anoxia recorded by the electrochemical sensor and the Winkler method (Figure 3a). On 16 March , nitrate concentrations in the bottom layer decreased from 21 to 3.1 μmol/L between 2:42 a.m. (Sta-127) and 10:03 p.m. (Sta-144) while nitrite concentrations increased from 0.59 to 11.2 μmol/L (Figure 3e). The following day, nitrate/nitrite concentrations reverted back to less extreme values (Figures 3d and 3e), but oxygen levels remained anomalously low at 5–13 μmol/kg (Figure 3a). The nitrogen deficit ($N^* = NO_3^- + NO_2^- - 16*PO_4^{3-}$) mirrors the nitrate/nitrite consumption/production (Figure 3f). The modest changes in phosphate concentration throughout the period indicate that ionic

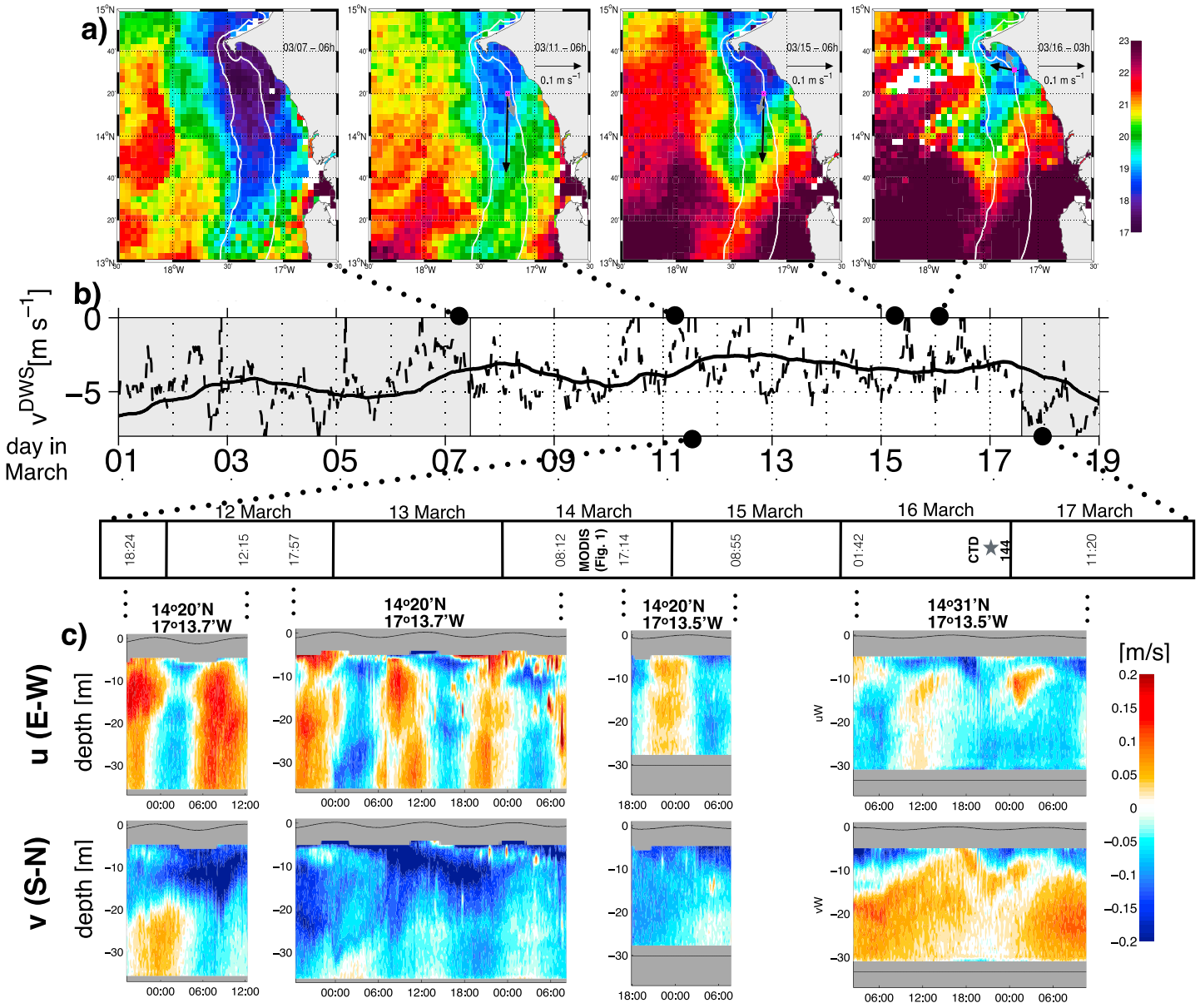

Figure 2. (a) Meteosat SEVIRI sea surface temperature (°C) at different times during UPSEN. Acoustic Doppler current profiler (ADCP) velocities over the bottom 15 m (resp. near-surface depth range 10 to 5 m) are indicated as black (resp. gray) vectors. Velocities are time averaged as in Figure 1c (velocities measured on 12–14 March are shown with sea surface temperature on 11 March). ADCP mooring sites also as in Figure 1c; (b) instantaneous (dashed) and low-pass filtered with one inertial period forward shift (solid black) meridional wind (m/s; negative is southward) at DWS (14°44′N, 17°30′W, 27 m above ground). Gray rectangles delineate the periods without shipboard measurements. The prolonged relaxation period is clearly visible between 7 and 17 March; (c) Midshelf time-depth diagrams of zonal (top) and meridional (bottom) currents (m/s) measured by upward ADCPs. The thin black lines near 0-m depth represent sea level position. The four distinct mooring locations and associated measurement time periods are reported in the time line above each panel. The timeline also indicates when the MODIS image (Figure 1) was taken and when Sta-144 was made. The subsurface shelf flow reversed to northward during the final part of UPSEN (lowest right panel).

forms of nitrogen were depleted (Figure 3b). The 10-m layer over the sediment thus presented consistent conditions of extremely low oxygen and large negative N* during the 30-hr period. A slight Chl-a increase toward the bottom is also noticeable in the same depth range (Figure 3g). Diagnostic pigment analysis revealed a biomass composition strongly dominated by diatoms that represented 60% to 95% of the total biomass (Figure 3h). The pheophorbide-a pigment concentration peaked at Sta-134 (16 March, 12:22 pm) at 5-m depth. Near the bottom, highest concentrations were encountered at Sta-148, followed by Sta-144 (0.6 and 0.44 μmol/L, respectively; Figure 3i).

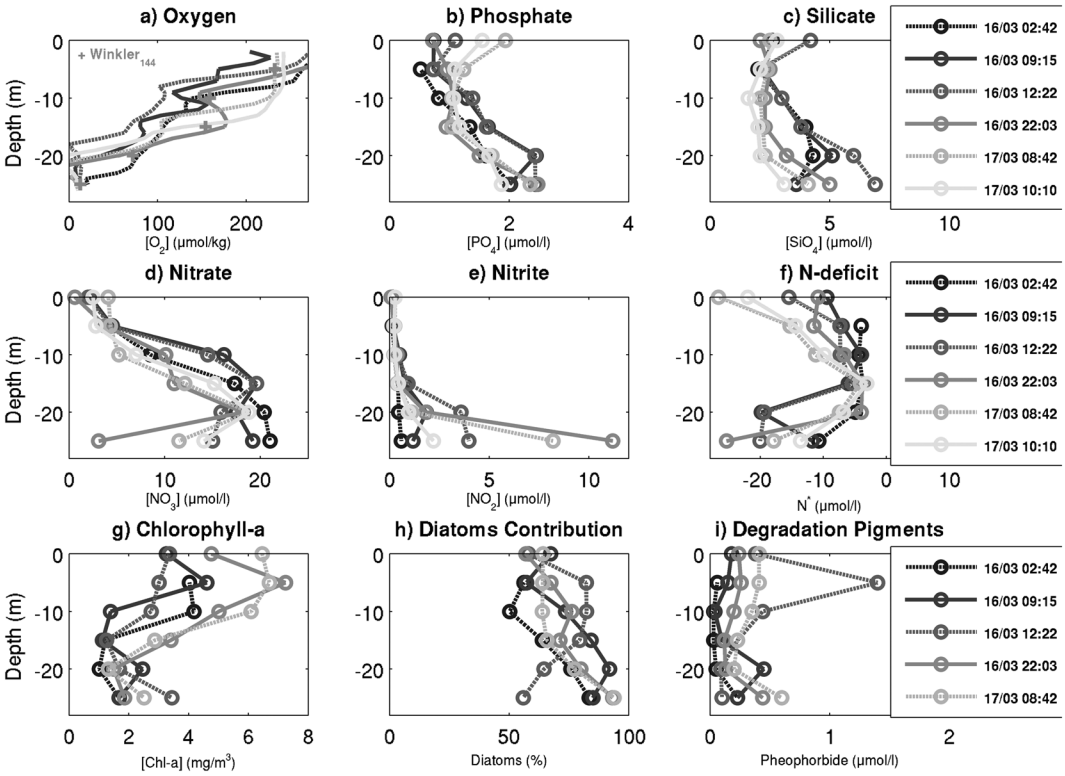

Figure 3. Profiles of (a) O2 concentrations from CTD casts, (b) phosphate, (c) silicate, (d) nitrate, (e) nitrite concentrations, and (f) nitrate deficit for stations 127 at 2:42 a.m., 130 at 9:15 a.m., 134 at 12:22 p.m., 144 at 22:03 on 16 March and stations 148 at 8:43 a.m., 152 at 10:10 a.m. the 17; profiles of (g) Chl-a, (h) diatom contribution to phytoplankton biomass, and (i) pheophorbide at the same stations 127, 130, 134, 144, and 148. Crosses in panel (a) correspond to Winkler oxygen measurements for Sta-144.

Figure 4 shows near-surface and near-bottom Chl-a concentrations, apparent oxygen utilization (AOU), and O2 concentrations at all field stations. The north-south distance between the observation sections is only 28 km (20 km between the central north and the northern sections), and the distribution of stations between shallow versus deep areas remained roughly constant throughout the experiment. Hence, we can present data shown in Figure 4 as mainly representative of temporal evolution over the entire area. O2 concentrations and AOU show that the midsurvey corresponded to the most productive phase at the surface (Figures 4b and 4c). The end of the survey is characterized by a reduction of O2 concentrations and an increase in AOU occurring at the same time, which reflects an enhanced respiration in surface waters. Over the whole survey, the bottom 5-m layer presented biomass ranging from few to 45 mgChl-a/m^2, the highest biomasses being measured for the section at 14°20′N (except for few single stations; Figure 4d). The most noticeable temporal changes concern near-bottom O2 and AOU that, respectively, exhibit a downward and an upward trend. These trends are particularly pronounced toward the end of the experiment when rapid changes seem to occur after Sta-130. The bottom O2 concentrations and AOU are less variable than in surface layers and show a continuous augmentation of consumption throughout UPSEN (Figures 4e and 4f). The 14°31′N section stands out with mean O2 falling below 10 µmol/kg for the bottom layer at several stations while AOU increases by ~30 µmol/kg. Note that bottom O2 concentrations at 14°20′N are statistically different from concentrations at 14°N and 14°31′N (*t* test at 95% confidence level) whereas concentrations at 14°N and 14°31′N are not.

4. Discussion

High-resolution sampling of the water column during UPSEN revealed a short episode of complete subsurface anoxia. Reaching the O2 levels observed at six stations situated within 1-km distance requires the consumption of ~60 µmol/kg of oxygen, this value being approximately the background concentration

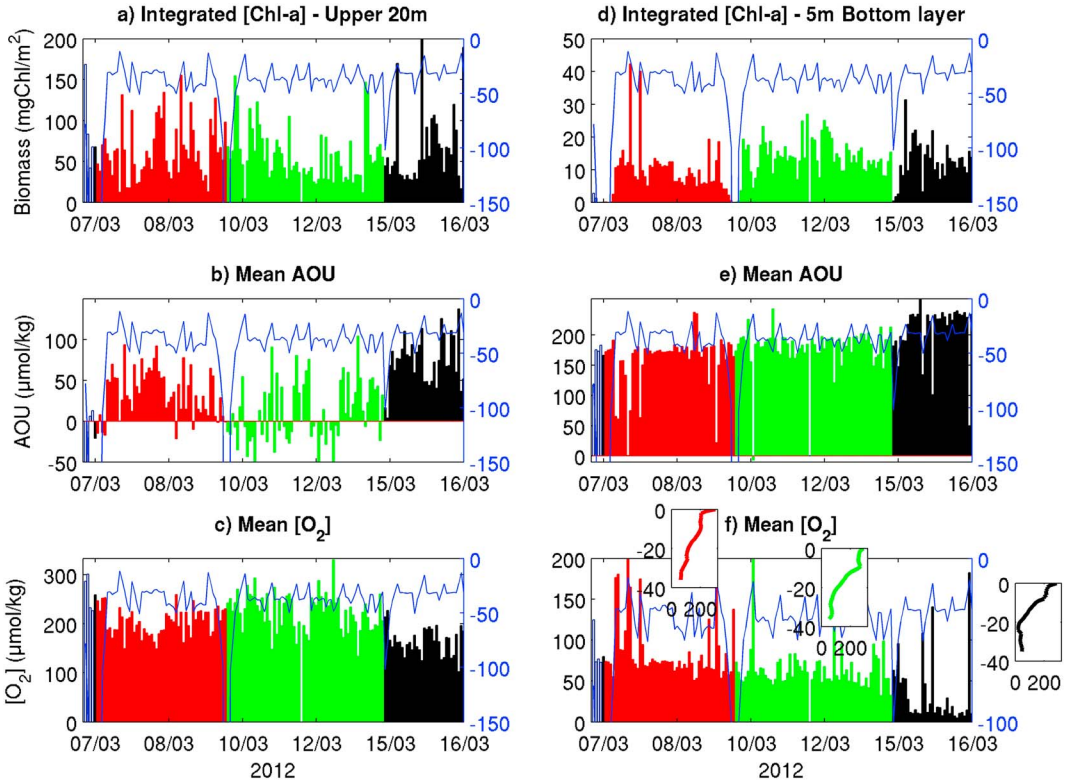

Figure 4. (a, d) Biomass, (b, e) mean apparent oxygen utilization ($[O2]_{sat}$-$[O2]_{mes}$), (c, f) and mean [O2] for the (a–c) upper layer (0–20 m) and the (d–f) bottom layer from CTD casts: 14°55′N (white), <14°06′N (red), 14°20′N (green), and 14°31′N (black). Right axis is the bathymetry (m) for each station displayed as a thin blue line on all panels (a–f). Mean O2 profiles for stations shallower than 45 m along transects at 14°N (red), 14°20′N (green), and 14°31′N (black) are added in panel (f).

for near-bottom upwelling waters over the southern Senegalese shelf (see Figure 4 in Capet et al., 2017). Ignoring processes other than local phytoplankton degradation and assuming a photosynthesis/respiration reaction with a typical mean carbon:chlorophyll ratio of 50, such reduction requires 10 mgChl-a/m^3. This Chl-a concentration was rarely encountered in places shallower than 20-m depth, except at ~14°20′N to 17°15′W toward the end of the survey (13 March, not shown). In practice, the observed O2 drawdown must have implied sinking of near-surface plankton in the bottom layer where degradation took place. In a 1-D vertical framework, required Chl-a concentrations are not fundamentally different because the surface layer where most of the plankton resides and the anoxic bottom layer have a similar thickness. Chl-a concentrations in the vicinity of the anoxia event were thus three to five times lower than the required 10 mgChl-a/m^3 (Figure 3g).

The presence of elevated Chl-a levels over the inner shelf and the sudden shift of the flow direction from equatorward to poleward at mid-shelf on 15 March potentially drove the development of the midshelf anoxic event. Chl-a concentrations of 10 mgChl-a/m^3 were present when anoxia occurred and shortly before with 16.9 mgChl-a/m^3 obtained by high-performance liquid chromatography at the surface for the inner-shelf Sta-128 (14°31′N to 17°10′W; 23-m depth) on 16 March. Chl-a patterns for 14 March are visible on MODIS image and confirm the widespread presence of elevated Chl-a nearshore and particularly inshore of the anoxic area (Figure 1). The comparison with estimates from in situ observations gives some confidence on the patterns and absolute numbers (mean Chl-a difference between satellite and HPCL measurements was 0.13 mgChl-a/m^3 for 14 March; Figure S1).

The observed anoxic event occurred toward the end of a prolonged upwelling relaxation phase that was particularly marked after 11 March (Figure 2). Current measurements indicate that the midshelf subinertial flow remained predominantly oriented toward the south during that period but reversed to northward on 15 March, that is, shortly before the anoxic event was observed (Figures 1 and 2). Synoptic fluctuations of

the local wind were limited around the time of flow reversal (Figure 2b). Thus, the most plausible explanation for this change in flow orientation involves remote wind fluctuations triggering coastal trapped waves, as classically found in coastal upwelling systems (Brink, 1991; Chapman, 1987; Hormazabal et al., 2004; Pringle & Dever, 2009). Although diabatic processes may be responsible for some of the SST differences between the SEVIRI scenes for 15 and 16 March (Figure 2a), the SST evolution between these dates is supportive of a shelf-scale flow reversal that would modify the shape of the cold upwelling plume (oriented north-south on 15 March and having a more tilted comma-type appearance on 16 March). Due to geomorphology of the shelf south Dakar, the circulation associated with coastal trapped waves cannot be purely meridional because it must roughly follow the isobaths (Wilkin & Chapman, 1990), hence the explanation for the orientation of the flow near the anoxic site on 16 March (Figure 1). This led to the transport of nearshore waters toward the mooring area (Figures 1 and 2).

Consumption of 45 to 60 μmol/kg of oxygen (near-bottom concentrations encountered at midshelf at 14°20′ N and in offshore upwelling waters, respectively) and over 20 mmol/m^3 of fixed nitrogen is unlikely to have taken place over a 24-hr period. This would imply extreme consumption rates of the order of 60 mmol/m^3/day, which are 2 orders of magnitude higher than typical respiration rates measured in upwelling regions (e.g., Adams et al., 2013). Accordingly, ocean currents must have mainly been responsible for advecting nearshore waters already highly depleted in O2 that had not been previously sampled, as opposed to suddenly creating conditions that would have led to rapid local O2 consumption near the anoxic site.

The origin of these O2-depleted waters cannot be precisely determined, but sustained O2 depletion can only have occurred (i) where biomass levels were sufficiently high to produce significant consumption, typically inshore of the 20- to 25-m isobath (Figure 1), and (ii) where the water depth was sufficient to prevent bottom water aeration through vertical mixing, that is, typically where the water column was stratified. The water column was always stratified at the stations we sampled (offshore of the 15-m isobaths), but nighttime wind speeds measured by the ship weather station systematically reached 15 knots (not shown), so significant O2 depletion may have been limited to beyond the 10-m isobath. The reduced size of the sector compatible with the production of near anoxic waters in the proposed scenarios is qualitatively consistent with the short duration of the anoxic event on 16 March. Several elements indicate that significant organic matter degradation and O2 consumption were occurring in the water column on 16 March.

Offshore stations along the 14°31′N transect presented surface and bottom maxima of Chl-a that supports the remote sedimentation of phytoplankton biomass mainly composed of diatoms and the advection of enriched phytoplankton in the vicinity of Sta-144 (Figures 3g and 3h). Decay rates tend to follow the overall biological richness of the water with the fastest decay occurring in rich nearshore waters (Fuhrman, 1999). Pheophorbide-a is usually considered as a product of Chl-a degradation associated to protozoan grazing (Lampert, 2001), which must have been active on 16 March when Pheophorbide-a concentrations are about three times higher than those found during the rest of the survey (Figure 3i; the average concentration during UPSEN was 0.17 μmol/L).

Nitrogen and O2 consumptions occurred at the sediment interface in our area of investigation (Dale et al., 2014; Sokoll et al., 2016) and can exhibit high temporal dynamics (Berg et al., 2013). At seasonal timescale, O2 consumption at the sediment interface was estimated to account for 16% of the 0.9 ml/L seasonal draw down over the Oregon shelf (Adams et al., 2013). According to Huettel et al. (2014), the highly permeable carbonate sand that constitutes the seabed in our area of investigation (Barusseau, 1984) can be a net source of O2 owing to high benthic photosynthesis rates. Measurements off Mauritania by 50-m depth during the upwelling season gave uptake rates of ~10 mmolO_2/m^2/day (Dale et al., 2014). Therefore, the underlying permeable sediments may play a role in the net oxygen demand in the lower 10 m of the water column, but flux intensity and direction are totally unconstrained in our observations.

The anoxia encountered at midshelf during an upwelling relaxation is thus the likely consequence of the advection of a decaying diatom bloom that developed in shallower waters. Similar sequences are also encountered in the Benguela and California upwelling systems (Chapman & Shannon, 1985; Checkley & Barth, 2009; Pitcher & Probyn, 2010, 2011).

Although nitrification is thought to be the main process producing the potent N_2O greenhouse gas off Mauritania (Kock et al., 2012), our study suggests that N_2O could be produced by denitrification in the

broader CCS. Production of N_2O through denitrification is thought to be favored compared to free nitrogen in coastal environments (Naqvi et al., 2006). Understanding oxygen dynamics over the southern Senegal shelf would be useful to quantify the CCS contribution to atmospheric concentration of this greenhouse gas.

Major unknowns remain regarding the duration and extension of the anoxia, the frequency of occurrence and regional consequences on the nitrogen budget and the ecosystem, including through possible export of low O2 waters toward the open ocean (Schütte et al., 2016). Note that nitrite can be poisonous for certain species. Coastal processes implicated in the production of local O2-depleted waters may be anthropogenically affected. This could add to or even surpass the concerns associated with the O2 trends in OMZs (Stramma et al., 2008). Additional observations as well as modeling will strive to fill these important knowledge gaps. Setting up a regular monitoring program will certainly be needed in order to understand O2 variability and the long-term evolution of low oxygen events and reveal the processes underlying regional changes in the OMZ and at local scales, such as the impacts of wastewater discharges around Dakar (Diop et al., 2014).

Acknowledgments
The present work was supported by AWA (01DG12073E, http://www.awa-project.org), FP7 PREFACE (603521, http://preface.b.uib.no), and the International joint Laboratory ECLAIRS (http://www.ird.fr/infos-pratiques/archives/anciens-lmi/lmi-eclairs-etude-du-climat-en-afrique-de-l-ouest). DWS Wind data are available from the Ogimet website (http://www.ogimet.com/metars.phtml.en). EUMETSAT Satellite Application Facility on Ocean and Sea Ice data used in this study are accessible through the SAF's homepage (http:///www.osi-saf.org/). Other data sets (oxygen, CTD, nutrients, currents, ad hoc MODIS image) used in this study are assigned the DOI 10.5281/zenodo.1324408. We thank the reviewers for their very constructive comments, which greatly helped to improve the manuscript. Finally, we thank Todd Capson for his careful proofreading.

References

Adams, K. A., Barth, J. A., & Chan, F. (2013). Temporal variability of near-bottom dissolved oxygen during upwelling off central Oregon. *Journal of Geophysical Research: Oceans*, *118*, 4839–4854. https://doi.org/10.1002/jgrc.20361

Aiken, J., Pradhan, Y., Barlow, R., Lavender, S., Poulton, A., Holligan, P., & Hardman-Mountford, N. (2009). Phytoplankton pigments and functional types in the Atlantic Ocean: A decadal assessment, 1995–2005. *Deep Sea Research Part II: Topical Studies in Oceanography*, *56*, 899–917. https://doi.org/10.1016/j.dsr2.2008.09.017

Aminot, A., & Kérouel, R. (2004). *Hydrologie des écosystèmes marins: paramètres et analyses*. Editions Quae, Versailles.

Arístegui, J., Barton, E. D., Álvarez-Salgado, X. A., Santos, A. M. P., Figueiras, F. G., Kifani, S., et al. (2009). Sub-regional ecosystem variability in the Canary Current upwelling. *Progress in Oceanography*, *83*(1–4), 33–48. https://doi.org/10.1016/j.pocean.2009.07.031

Barusseau, J.P. (1984). Analyse sédimentologique des fonds marins de la "petite côte" (Sénégal), Document scientifique n° 94, ISSN 0850-1602.

Berg, P., Long, M. H., Huettel, M., Rheuban, J. E., McGlathery, K. J., Howarth, R. W., et al. (2013). Eddy correlation measurements of oxygen fluxes in permeable sediments exposed to varying current flow and light. *Limnology and Oceanography*, *58*, 1329–1343. https://doi.org/10.4319/lo.2013.58.4.1329

Brandt, P., Bange, H. W., Banyte, D., Dengler, M., Didwischus, S. H., Fischer, T., et al. (2015). On the role of circulation and mixing in the ventilation of oxygen minimum zones with a focus on the eastern tropical North Atlantic. *Biogeosciences*, *12*, 489–512. https://doi.org/10.5194/bg-12-489-2015

Breitburg, D., Levin, L. A., Oschlies, A., Grégoire, M., Chavez, F. P., Conley, D. J., et al. (2018). Declining oxygen in the global ocean and coastal waters. *Science*, *359*, eaam7240. https://doi.org/10.1126/science.aam7240

Brink, K. H. (1991). Coastal-trapped waves and wind-driven currents over the continental shelf. *Annual Review of Fluid Mechanics*, *23*(1), 389–412. https://doi.org/10.1146/annurev.fl.23.010191.002133

Capet, X., Estrade, P., Machu, E., Marié, L., Ndoye, S., Grelet, J., et al. (2017). The southern Senegal upwelling center: State and functioning during the UPSEN2/ECOAO field experiments (Feb.–Mar. 2013). *Journal of Physical Oceanography*, *47*, 155–180. https://doi.org/10.1175/JPO-D-15-0247.1

Caverivière, A., & Touré, D. (1990). Note sur les mortalités de mérou (Serranidae) observées en fin de saison chaude devant les côtes du Sénégal, particulièrement en 1987.

Chan, F., Barth, J. A., Lubchenco, J., Kirincich, A., Weeks, H., Peterson, W. T., & Menge, B. A. (2008). Emergence of anoxia in the California Current large marine ecosystem. *Science*, *319*(5865), 920–920. https://doi.org/10.1126/science.1149016

Chapman, D. C. (1987). Application of wind-forced, long, coastal-trapped wave theory along the California coast. *Journal of Geophysical Research*, *92*(C2), 1798–1816. https://doi.org/10.1029/JC092iC02p01798

Chapman, P., & Shannon, L. V. (1985). The Benguela ecosystem. Part II. Chemistry and related processes. *Oceanography and Marine Biology: An Annual Review*, *23*, 183–251.

Checkley, D. M. Jr., & Barth, J. A. (2009). Patterns and processes in the California Current System. *Progress in Oceanography*, *83*(1–4), 49–64. https://doi.org/10.1016/j.pocean.2009.07.028

Cockcroft, A. C. (2001). Jasus lalandii 'walkouts' or mass strandings in South Africa during the 1990s: An overview. *Marine and Freshwater Research*, *52*(8), 1085–1093. https://doi.org/10.1071/MF01100

Codispoti, L. A., & Christensen, J. P. (1985). Nitrification, denitrification and nitrous oxide cycling in the eastern tropical South Pacific Ocean. *Marine Chemistry*, *16*(4), 277–300. https://doi.org/10.1016/0304-4203(85)90051-9

Dale, A. W., Sommer, S., Ryabenko, E., Noffke, A., Bohlen, L., Wallmann, K., et al. (2014). Benthic nitrogen fluxes and fractionation of nitrate in the Mauritanian oxygen minimum zone (Eastern Tropical North Atlantic). *Geochimica et Cosmochimica Acta*, *134*, 234–256. https://doi.org/10.1016/j.gca.2014.02.026

Diaz, R. J., & Rosenberg, R. (2008). Spreading dead zones and consequences for marine ecosystems. *Science*, *321*(5891), 926–929. https://doi.org/10.1126/science.1156401

Diop, C., Dewaelé, D., Diop, M., Touré, A., Cabral, M., Cazier, F., et al. (2014). Assessment of contamination, distribution and chemical speciation of trace metals in water column in the Dakar coast and the Saint Louis estuary from Senegal, West Africa. *Marine Pollution Bulletin*, *86*(1-2), 539–546. https://doi.org/10.1016/j.marpolbul.2014.06.051

Diouf, D., Niang, A., Brajard, J., Crepon, M., & Thiria, S. (2013). Retrieving aerosol characteristics and sea-surface chlorophyll from satellite ocean color multi-spectral sensors using a neural-variational method. *Remote Sensing of Environment*, *130*, 74–86. https://doi.org/10.1016/j.rse.2012.11.002

Fuhrman, J. A. (1999). Marine viruses and their biogeochemical and ecological effects. *Nature*, *399*(6736), 541–548. https://doi.org/10.1038/21119

Glessmer, M. S., Eden, C., & Oschlies, A. (2009). Contribution of oxygen minimum zone waters to the coastal upwelling off Mauritania. *Progress in Oceanography*, *83*(1–4), 143–150. https://doi.org/10.1016/j.pocean.2009.07.015

Grantham, B. A., Chan, F., Nielsen, K. J., Fox, D. S., Barth, J. A., Huyer, A., et al. (2004). Upwelling-driven nearshore hypoxia signals ecosystem and oceanographic changes in the northeast Pacific. *Nature*, *429*(6993), 749–754. https://doi.org/10.1038/nature02605

Hernández-Miranda, E., Quiñones, R. A., Aedo, G., Valenzuela, A., Mermoud, N., Román, C., & Yañez, F. (2010). A major fish stranding caused by a natural hypoxic event in a shallow bay of the eastern South Pacific Ocean. *Journal of Fish Biology*, *76*, 1543–1564. https://doi.org/10.1111/j.1095-8649.2010.02580.x

Hormazabal, S., Shaffer, G., & Leth, O. (2004). Coastal transition zone off Chile. *Journal of Geophysical Research*, *109*, C01021. https://doi.org/10.1029/2003JC001956

Huettel, M., Berg, P., & Kostka, J. E. (2014). Benthic exchange and biogeochemical cycling in permeable sediments, *Annual Review of Marine Science*; *6*, 23-51. https://doi.org/10.1146/annurev-marine-051413-012706

Klenz, T., Dengler, M., & Brandt, P. (2018). Seasonal variability of the Mauritania Current and hydrography at 18 N. *Journal of Geophysical Research: Oceans*, *123*, 8122–8137. https://doi.org/10.1029/2018JC014264

Kock, A., Schafstall, J., Dengler, M., Brandt, P., & Bange, H. W. (2012). Sea-to-air and diapycnalnitrous oxide fluxes in the eastern tropical North Atlantic Ocean. *Biogeosciences (BG)*, *9*, 957–964. https://doi.org/10.5194/bg-9-957-2012

Kounta, L., Capet, X., Jouanno, J., Kolodziejczyk, N., Sow, B., & Thierno Gaye, A. (2018). A model perspective on the dynamics of the shadow zone of the eastern tropical North Atlantic–Part 1: The poleward slope currents along West Africa. *Ocean Science*, *14*, 971–997. https://doi.org/10.5194/os-14-971-2018

Kuypers, M. M., Lavik, G., Woebken, D., Schmid, M., Fuchs, B. M., Amann, R., et al. (2005). Massive nitrogen loss from the Benguela upwelling system through anaerobic ammonium oxidation. *Proceedings of the National Academy of Sciences of the United States of America*, *102*(18), 6478–6483. https://doi.org/10.1073/pnas.0502088102

Lampert, L. (2001). Dynamique saisonnière et variabilité pigmentaire des populations phytoplanctoniques dans l'Atlantique Nord (Golfe de Gascogne). Doctoral dissertation, Université de Bretagne Occidentale.

Monteiro, P. M., & van der Plas, A. K. (2006). Low oxygen water (LOW) variability in the Benguela system: Key processes and forcing scales relevant to forecasting. *Large Marine Ecosystems*, *14*, 71–90. https://doi.org/10.1016/S1570-0461(06)80010-8

Morison, J., Andersen, R., Larson, N., D'Asaro, E., & Boyd, T. (1994). The correction for thermal-lag effects in Sea-Bird CTD data. *Journal of Atmospheric and Oceanic Technology*, *11*(4), 1151–1164. https://doi.org/10.1175/1520-0426(1994)011<1151:TCFTLE>2.0.CO;2

Naqvi, S. W. A., Naik, H., Pratihary, A., D'Souza, W., Narvekar, P. V., Jayakumar, D. A., et al. (2006). Coastal versus open-ocean denitrification in the Arabian Sea. *Biogeosciences*, *3*(4), 621–633. https://doi.org/10.5194/bg-3-621-2006

Ndoye, S. (2016). Fonctionnement dynamique du centre d'upwelling Sud-Sénégalais: approche par la modélisation réaliste et l'analyse d'observations satellite de température de surface de la mer. Doctoral dissertation, Université Pierre et Marie Curie-Paris VI.

Ndoye, S., Capet, X., Estrade, P., Sow, B., Dagorne, D., Lazar, A., et al. (2014). SST patterns and dynamics of the Southern Senegal-Gambia upwelling center. *Journal of Geophysical Research: Oceans*, *119*, 8315–8335. https://doi.org/10.1002/2014JC010242

Ndoye, S., Capet, X., Estrade, P., Sow, B., Machu, E., Brochier, T., et al. (2017). Dynamics of a low enrichment-high retention upwelling center over the southern Senegal shelf. *Geophysical Research Letters*, *44*, 5034–5043. https://doi.org/10.1002/2017GL072789

Pitcher, G. C., & Probyn, T. A. (2010). Red tides and anoxia: An example from the southern Benguela current system. KALLIOPI A. PAGOU, 159.

Pitcher, G. C., & Probyn, T. A. (2011). Anoxia in southern Benguela during the autumn of 2009 and its linkage to a bloom of the dinoflagellate Ceratium balechii. *Harmful Algae*, *11*, 23–32. https://doi.org/10.1016/j.hal.2011.07.001

Pringle, J. M., & Dever, E. P. (2009). Dynamics of wind-driven upwelling and relaxation between Monterey Bay and Point Arena: Local-, regional-, and gyre-scale controls. *Journal of Geophysical Research*, *114*(C7). https://doi.org/10.1029/2008JC005016

Rabalais, N. N., Diaz, R. J., Levin, L. A., Turner, R. E., Gilbert, D., & Zhang, J. (2010). Dynamics and distribution of natural and human-caused hypoxia. *Biogeosciences*, *7*, 585–619. https://doi.org/10.5194/bg-7-585-2010

Ras, J., Uitz, J., & Claustre, H. (2008). Spatial variability of phytoplankton pigment distributions in the Subtropical South Pacific Ocean: Comparison between in situ and modelled data. *Biogeosciences*, *5*(2), 353–369. https://doi.org/10.5194/bg-5-353-2008

Sarmiento, J. L., & Gruber, N. (2006). *Ocean biogeochemical dynamics* (p. 528). Hardcover: Pinceton University Press. 9780691017075

Schütte, F., Karstensen, J., Krahmann, G., Hauss, H., Fiedler, B., Brandt, P., et al. (2016). Characterization of "dead-zone" eddies in the eastern tropical North Atlantic. *Biogeosciences*, *13*, 5865–5881. https://doi.org/10.5194/bg-13-5865-2016

Sokoll, S., Lavik, G., Sommer, S., Goldhammer, T., Kuypers, M. M., & Holtappels, M. (2016). Extensive nitrogen loss from permeable sediments off North-West Africa. *Journal of Geophysical Research: Biogeosciences*, *121*, 1144–1157. https://doi.org/10.1002/2015JG003298

Stramma, L., Johnson, G. C., Sprintall, J., & Mohrholz, V. (2008). Expanding oxygen-minimum zones in the tropical oceans. *Science*, *320*(5876), 655–658. https://doi.org/10.1126/science.1153847

Van Heukelem, L., & Thomas, C. S. (2001). Computer-assisted high-performance liquid chromatography method development with applications to the isolation and analysis of phytoplankton pigments. *Journal of Chromatography A*, *910*(1), 31–49. https://doi.org/10.1016/S0378-4347(00)00603-4

Vaquer-Sunyer, R., & Duarte, C. M. (2008). Thresholds of hypoxia for marine biodiversity. *Proceedings of the National Academy of Sciences*, *105*(40), 15,452–15,457. https://doi.org/10.1073/pnas.0803833105

Wilkin, J. L., & Chapman, D. C. (1990). Scattering of coastal-trapped waves by irregularities in coastline and topography. *Journal of Physical Oceanography*, *20*(3), 396–421. https://doi.org/10.1175/1520-0485(1990)020<0396:SOCTWB>2.0.CO;2

Zhang, H.-M., Bates, J. J., & Reynolds, R. W. (2006). Assessment of composite global sampling: Sea surface wind speed. *Geophysical Research Letters*, *33*, L17714. https://doi.org/10.1029/2006GL027086

Zhang, J., Gilbert, D., Gooday, A., Levin, L., Naqvi, S. W. A., Middelburg, J. J., et al. (2010). Natural and human-induced hypoxia and consequences for coastal areas: Synthesis and future development. *Biogeosciences*, *7*, 1443–1467. https://doi.org/10.5194/bg-7-1443-2010